Visual Interpretation of Polarimetric SAR Imagery

A.C. van den Broek[*a], A.J.E. Smith[*a], A. Toet[**b]
[a]TNO Physics and Electronics Laboratory; [b]TNO Human Factors

ABSTRACT

A study is presented in which several different representations of polarimetric SAR data for visual interpretation are evaluated. Using a group of observers the tasks 'land use classification' and 'object detection' were examined. For the study, polarimetric SAR data were used with a resolution of 3 meters. These data were obtained with the Dutch PHARUS sensor from two test areas in the Netherlands. The land use classes consisted of bare soil, water, grass, urban and forest. The objects were farmhouses. It was found that people are reasonably successful in performing land use classification using SAR data. Multi-polarised data are required, but these data need not to be fully polarimetric, since the best results were obtained with the *hh*- and *hv*-polarisation combinations displayed in the red and green colour channels. Detection of objects in SAR imagery by visual inspection is very difficult. Most representations gave minimal results. Only when the *hh*- and *hv*-polarisation combinations were displayed in the red and green channels, somewhat better results were obtained. Comparison with an automatic classification procedure showed that land use classification by visual inspection appears to be the more effective. Automatic detection of objects gave better results than by visual inspection, but many 'false' objects were also detected.

Keywords: SAR, polarimetry, visualisation, classification, detection

1. INTRODUCTION

Visual interpretation of optical and thermal infrared imagery has been evolving over many years resulting in standard techniques. Due to its different physical nature SAR imagery shows a number of distinct aspects which hinder human interpretation. Examples are speckle noise due to the coherent character of the microwave radiation and specular reflections from objects. Polarimetric SAR imagery offers more information compared to single channel SAR imagery. The polarimetric information can be used to filter the imagery in order to reduce the speckle noise or to display the image in different colour channels offering more possibilities to the human eye to discriminate image objects. To investigate how polarimetric data can be optimally displayed for human interpretation we have conducted an experiment where observers were asked to classify different land use classes, and to detect objects in polarimetric SAR imagery. The imagery has been collected using the Dutch airborne PHARUS sensor of a suitable test site in the Netherlands. We used different image presentations reducing speckle in the imagery or adding colour to the imagery. The classification and detection results from the observers were used to evaluate which image presentation is the most effective for human interpretation.
The paper is organised as follows. First we give an overview of the various properties of polarimetric imagery and which of these properties can be used for displaying polarimetric information in order to enhance the visual presentation. Secondly we describe the test data and the experimental set-up, followed by a summary of the results from the experiment. We analyse and discuss these results and complete this paper with conclusions.

* vandenbroek@fel.tno.nl; phone: +31 70 374 0430; fax: +31 70 374 0654; a.j.e.smith@fel.tno.nl; phone: +31 70 374 0703; fax: +31 70 374 0654; TNO Physics and Electronics Laboratory, P.O. Box 96864, 2509 JG The Hague, The Netherlands.

** toet@tm.tno.nl ; phone: +31 3463 5 6237; fax: +31 3463 5 3977; TNO Human Factors, P.O. box 23, 3769 ZG Soesterberg, The Netherlands.

2. DISPLAYING POLARIMETRIC DATA

2.1 Polarimetric properties

Polarimetirc data consists of three independent measurements usually performed with vertical and horizontal polarised antennas. The measurement are given as complex scattering amplitudes in the vector format:

$$\vec{X} = \begin{pmatrix} S_{hh} \\ S_{hv} \\ S_{vv} \end{pmatrix} \tag{1}$$

The indices indicate the polarisation combination of the transmitting and receiving antennas. Because of reciprocity $S_{hv}=S_{vh}$, so that we only use S_{hv} for simplicity. The scattering coefficients are given by the matrix:

$$\vec{X}\vec{X}^{+} = \begin{pmatrix} \sigma_{hh} & \sigma_{hhhv} e^{i(\varphi_{hh}-\varphi_{v})} & \sigma_{hhvv} e^{i(\varphi_{hh}-\varphi_{vv})} \\ \sigma_{hvhh} e^{i(\varphi_{hv}-\varphi_{hh})} & \sigma_{hv} & \sigma_{hvvv} e^{i(\varphi_{hv}-\varphi_{vv})} \\ \sigma_{vvhh} e^{i(\varphi_{vv}-\varphi_{hh})} & \sigma_{vvhv} e^{i(\varphi_{vv}-\varphi_{hv})} & \sigma_{vv} \end{pmatrix} \tag{2}$$

where $\vec{X}^{+}$ denotes the complex conjugate of $\vec{X}$ so that e.g. $\sigma_{hh} = S_{hh}S_{hh}^{+}$ etc. When multilooking is applied, this matrix is averaged and the so-called polarimetirc covariance matrix with polarimetric correlation coefficients is obtained. For distributed targets the polarimetric covariance matrix C usually takes the following form:

$$C = \begin{pmatrix} \sigma_{hh} & 0 & \sigma_{hhvv} e^{i(\varphi_{hh}-\varphi_{vv})} \\ 0 & \sigma_{hv} & 0 \\ \sigma_{hhvv} e^{-i(\varphi_{hh}-\varphi_{vv})} & 0 & \sigma_{vv} \end{pmatrix} = \sigma_{hh} \begin{pmatrix} 1 & 0 & \rho\sqrt{\gamma} \\ 0 & \varepsilon & 0 \\ \rho^{*}\sqrt{\gamma} & 0 & \gamma \end{pmatrix} \tag{3}$$

where the co-cross correlation coefficients are assumed to be zero due to rotation symmetry[1] and where $\varepsilon=\sigma_{hv}/\sigma_{hh}$, $\gamma=\sigma_{vv}/\sigma_{hh}$ and ρ is the normalised correlation coefficient.
The polarimetric information can be used to reduce speckle in the image by applying the so-called Polarimetric Whitening Filter (PWF), which is given by:[2]

$$PWF = \frac{trace(C_{background}^{-1} C)}{3} \tag{4}$$

and where $C_{background}$ is a typical covariance matrix for the background and C is the covariance matrix of the pixel for which the PWF value has to be calculated.
If we assume azimuthal symmetry which usually holds for natural fields $\rho\sqrt{\gamma}=1-2\varepsilon$ and the σ_{hh} and σ_{vv} scattering coefficients are equal[1], implying that $\gamma=1$. In this case the PWF filter reduces to:

$$PWF = \sigma_{hh} + \frac{\sigma_{hv}}{\varepsilon} + \frac{|S_{vv} - (1-2\varepsilon)S_{hh}|^{2}}{1-(1-2\varepsilon)^{2}} \tag{5}$$

To calculate the PWF we have used $\varepsilon=0.2$, which is a nominal value for polarimetric covariance matrices like grass etc.

2.2 Polarimetric representations

As can be seen from equation (1) a polarimetric measurement consists of three separate measurements. Using the vector in equation (1) as basis we obtain quantities directly related to the way the sensor has measured. We call this the *sensor*

representation. In this representation a colour image can be obtained by displaying using the backscattering coefficients (σ_{hh}, σ_{hv}, σ_{vv}) in the red, green and blue channels, respectively.

Besides the *sensor* representation we can look for other representations, which resemble more closely the physical scatter mechanisms we expect to occur in the image. Typical scatter mechanisms are single bounce scattering, double bounce scattering and multi-bounce or volume scattering. A transformation of the vector in equation (1) to:

$$\vec{X} = \begin{pmatrix} (S_{hh} + S_{vv})/\sqrt{2} \\ S_{hv} \\ (S_{hh} - S_{vv})/\sqrt{2} \end{pmatrix} \approx \begin{pmatrix} Single \\ Multiple \\ Double \end{pmatrix} \tag{6}$$

provides a basis which resembles more closely the physical scatter mechanisms. For single bounce scattering the phase difference (φ_{hh}-φ_{vv}) is 0 degrees and for double bounce scattering (φ_{hh}-φ_{vv}) is 180 degrees. So using a plus and minus sign for the single and double bounce scattering, respectively, these scatter mechanisms are more prominent in the displayed image. Multiple bounce scattering changes the polarisation to a certain degree and therefore enhancing S_{hv}. We call this the *physical* representation. In this representation a colour image can be displayed analogously to the *sensor* representation by displaying the coefficients $(\sigma_{hh}+\sigma_{vv})/2+Re(\sigma_{hhvv})$, σ_{hv}, $(\sigma_{hh}+\sigma_{vv})/2-Re(\sigma_{hhvv})$ in the red, green and blue channels, respectively.

Another representation, the *eigenwaarde* representation, is given by three uncorrelated quantities obtained from the eigenvalues of the covariance matrix. Using the rotation symmetric covariance matrix (Equation 3) these eigenvalues are given by:

$$\begin{aligned} \sigma_1 &= \left(\frac{\sigma_{hh} + \sigma_{vv}}{2}\right) + \sqrt{\left(\frac{\sigma_{hh} - \sigma_{vv}}{2}\right)^2 + \sigma_{hhvv}^2} \\ \sigma_2 &= \sigma_{hv} \\ \sigma_3 &= \left(\frac{\sigma_{hh} + \sigma_{vv}}{2}\right) - \sqrt{\left(\frac{\sigma_{hh} - \sigma_{vv}}{2}\right)^2 + \sigma_{hhvv}^2} \end{aligned} \tag{7}$$

In this representation, obviously, a colour image can be displayed by using coefficients $(\sigma_1, \sigma_2, \sigma_3)$ in the red, green and blue channels, respectively.

2.3 Displaying of representations

Above mentioned representations can be used to construct grey tone and colour images. To do this we first take the logarithm of the quantities to be displayed following

$$\sigma(dB) = 10\log(\sigma) \tag{8}$$

and then determine the mean μ and the standard deviation *sd* of the image. Since in a colour channel only 255 intensity levels are available, we distribute the values in the interval (μ+2sd, μ-2sd) equally over the 255 intensity levels following:

$$\sigma_{(0-255)} = 255\frac{(\sigma(dB) - (\mu - 2sd))}{4sd} \tag{9}$$

In this way we have stretched the image to obtain optimal contrast on the screen when grey tone images like single channel images and PWF images are displayed. For the colour images we display the three quantities in the red, green and blue colour channels, where we have stretched the quantities in the different colour channels independently following the above mentioned procedure.

When only two quantities are to be displayed we use the red and green colour channels and leave the blue channel empty. The reason is that the human eye is more sensitive to green and red light than to blue light and thus sees more intensity levels in these channels.

2.4 Test data

For this study we used polarimetric SAR data from the Dutch PHARUS sensor. With this C-band SAR sensor, images were collected with a resolution of about 3 meter, 5 looks and with incidence angles between 50 and 70 degrees. The calibration procedure consisted of phase calibration, cross-talk removal, and channel imbalance. No absolute calibration was performed.
The test site used is located in the eastern part of the Netherlands, near the river IJssel and just North of the city Deventer. The area consists of various 'culture' landscapes showing forest parcels, agricultural fields, urban areas, scattered farmhouses, water and grassland.
We selected two areas of 3 by 3 km, one with an urban area and one where only farmhouses are present. The first area was used for experiment A (land use classification), while the second area was used for experiment B (object detection). In Figure 1 we show PWF images of both areas.

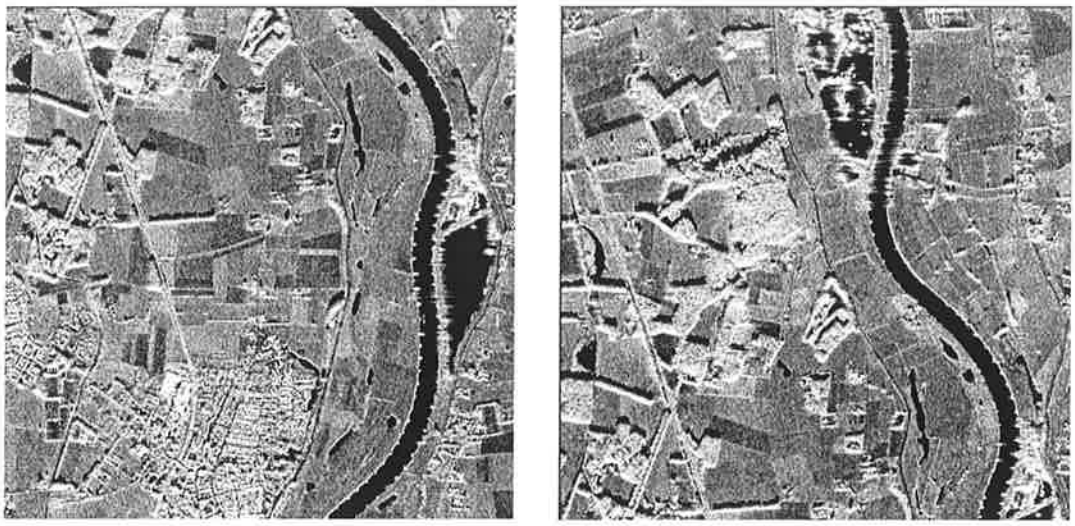

Figure 1. PWF images of the areas used in experiment A (left) and experiment B (right).

For these areas also multi-spectral optical data with a resolution of 3 meter were available. The data consisted of three bands in the near-infrared, red and green part of the optical spectrum and are especially useful to determine the characteristics of vegetated areas versus non-vegetated areas. The optical data were used as 'ground truth' to construct reference templates (see Figure 2) for comparing the classification and detection results from the observers.

We showed the observers 4 representations of the scenes summarised here in the following Table.

Table 1. Representations used in the experiments

representation	no. of channels	coefficients	no. of observers
hh	one channel image	σ_{hh}	11
pwf	one channel speckle reduced image	σ_{pwf}	13
hhhv	two colour channel image	σ_{hh}, σ_{hv}	12
pol	a three colour channel image	σ_{hh}, σ_{hv}, σ_{vv}	11

For each representation the scattering coefficients, which are dislayed, are shown in the third column. For practical reasons we could only study one of the three polarimetric representations described in section 2.2. We prepared all three representations. A visual comparison made by the authors did not show much distinction between the *physical* and *eigenwaarde* representation. In fact the *sensor* representation showed more colour tints than the other two representations. Therefore, we have chosen to use this representation and evaluate the other representations at a later stage.
For the two-colour representation, we have used a co-polarised backscatter coefficient (σ_{hh}) and a cross-polarised backscatter coefficient (σ_{hv}). The advantage of this combination is that these scattering coefficients are usually not correlated for natural targets[1] and can be measured with one transmitting and two receiving antennas.

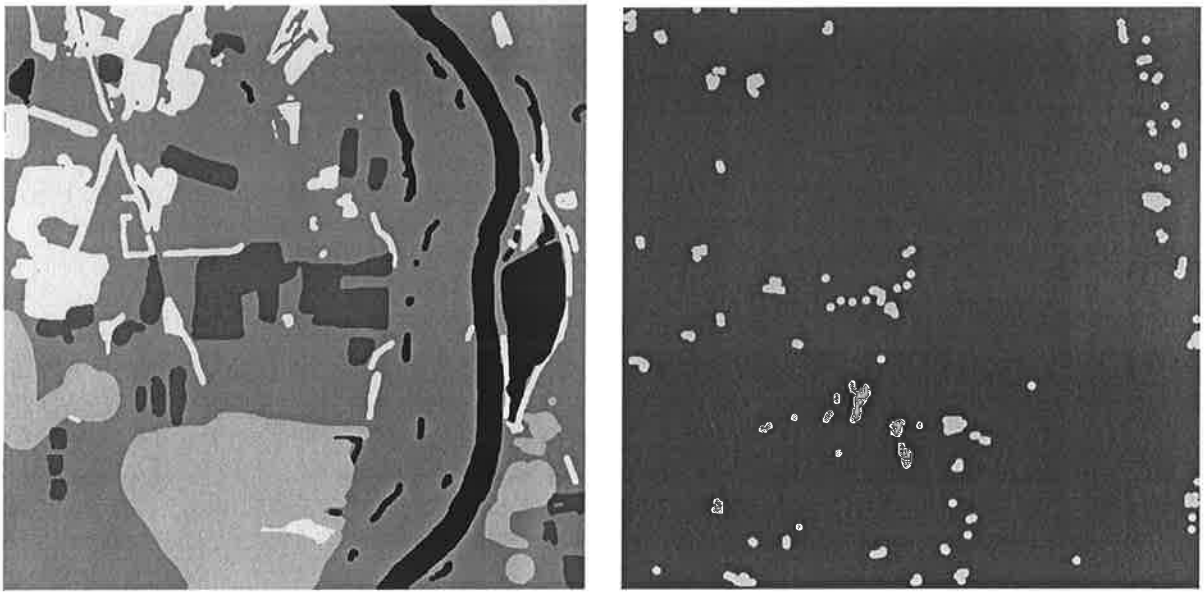

Figure 2. Reference template for experiment A is shown at the left. This template shows 5 land use classes (in the order dark to bright: water, bare soil, grass, urban, forest). Reference template for experiment B is shown at the right. In this template buildings complexes are bright.

3. EXPERIMENT

3.1 Experimental set-up

The total experiment consisted of two main parts: land use classification (experiment A) and object detection (experiment B), where the different representation were shown to the observers on a PC monitor. Both in experiment A and B the four image representations shown in Table 1 were used. For each image representation a group consisting of 11-13 observers (see Table 1) was selected. Each group was asked using a digital pen to colourize the land use classes (experiment A), and the building complexes (experiment B). For this purpose the Adobe Photoshop software package on a standard PC was used. For experiment A, observers were asked to mark the following land use categories: water, urban area, forest and bare soil. The rest of the area in the scene, the background, was considered to be grass. For experiment B observers were asked within a certain time limit to indicate building complexes like farmhouses. In total 75 of such complexes were present in the scene. The group of observers consisted of persons not familiar with SAR imagery. In order to make the observers familiar with SAR imagery they were first trained by showing and explaining SAR images of the same representation, as they had to use in the experiments. Of course, the areas shown, differed from the ones used in the experiments, but showed similar land use classes and building complexes.

3.2 Experiment results

From each of the observers two templates were collected, one from experiment A and one from experiment B. We wanted to evaluate which representation is most suitable for human interpretation for an average group of people. To prevent that individual mistakes can influence the result we have calculated 'average' observer templates for each representation and experiment, so that in total 8 templates were obtained. These 'average' observer templates show only those classifications, which are confirmed by a majority (i.e. 50% or more) of the group of observers. If this is not the case the class 'confused' was taken. For illustration observer templates for the representation *hh* and *pol* from experiment A are shown in Figure 3. Clearly visible in the Figure is that the *hh* template shows more confusion and less bare soil compared to the *pol* template.

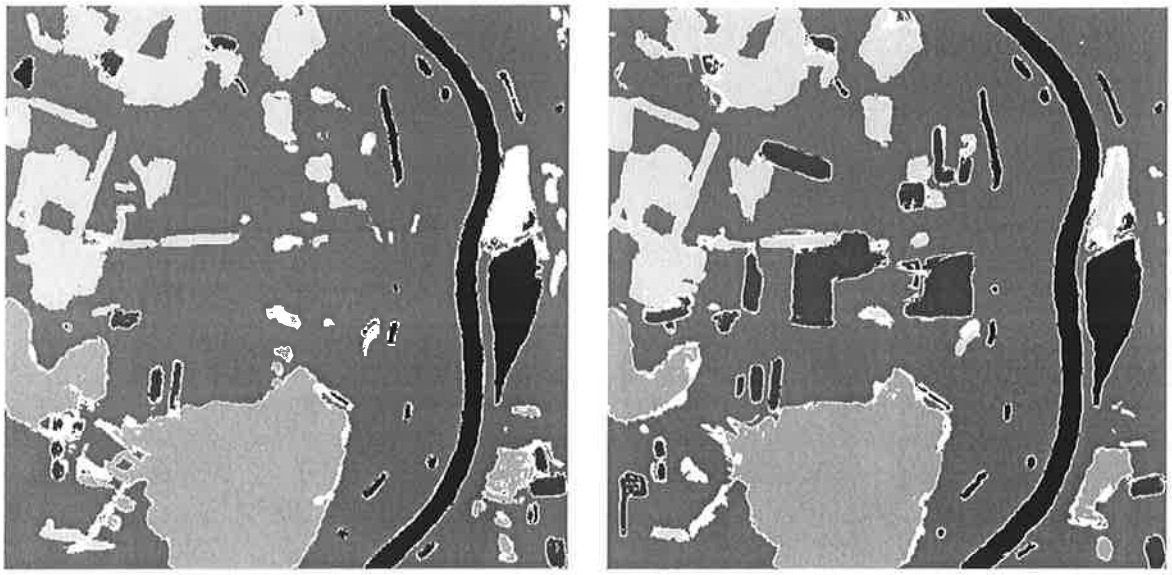

Figure 3. Observer templates from experiment A. The template for the *hh* representation (left) and the *pol* representation are shown (right). Confusion is shown in white. Land use classes as in Figure 2.

The observer templates were then compared with the reference templates (see Figure 2). General properties of the templates from experiment A are given in Table 2. In case of experiment A we calculated confusion matrices (see Table 3) from the comparison indicating the relative percentages of correctly and incorrectly classified land use classes. We also give an average percentage of correct classification. In case of experiment B we simply counted the number of objects found (see Table 4).

Table 2. Relative percentages of the areas of the land use classes in the various templates

Experiment A	bare soil	Water	urban	grass	Forest	confused
ref. template	7	9	13	60	11	-
hh	1	6	12	63	8	9
pwf	4	6	14	57	9	10
hhhv	6	7	13	61	10	3
Pol	5	7	11	60	9	8

Table 3. Confusion matrices for the different representations in experiment A

hh	bare soil	Water	Urban	grass	Forest	confused
Bare soil	13	0	0	79	0	8
Water	0	69	0	16	0	15
Urban	0	0	83	10	0	7
Grass	0	0	2	87	3	8
Forest	0	0	2	22	61	14
Average correct 63%						

Pwf	Bare soil	Water	Urban	grass	Forest	confused
Bare soil	46	0	0	38	1	15
Water	0	70	1	12	0	17
Urban	0	0	88	7	0	5
Grass	1	1	3	84	3	9
Forest	0	0	3	17	66	14
Average correct 71%						

Hhhv	Bare soil	water	Urban	grass	forest	confused
Bare soil	69	0	0	24	1	6
Water	0	75	1	17	0	7
Urban	0	0	84	13	0	2
Grass	2	1	2	89	3	2
Forest	0	0	3	26	67	3
Average correct 77%						

Pol	bare soil	water	Urban	grass	Forest	confused
Bare soil	61	0	0	22	0	17
Water	0	72	0	16	0	12
Urban	0	0	81	12	0	7
Grass	1	1	1	88	3	6
Forest	0	0	2	24	63	11
Average correct 73%						

Table 4. Number of objects detected by a majority of the observers.

Experiment B	No. of objects	Rel. percentage
ref. Template	75	100
Hh	1	1
Pwf	8	11
Hhhv	20	27
Pol	6	8

Note that all detected objects in Table 4 were present in the reference template so that no 'false' objects were detected. All 6 objects from the *pol* representation were also found in the *hhhv* representation. On the other hand, 4 objects in the *pwf* representation and the one object in the *hh* representation were not found in the *hhhv* representation.

4. ANALYSIS

An inspection of the images presented to the observers, shows that the single polarised images are rather noisy compared to the PWF images. This is due to reduction of the speckle noise in the PWF image by averaging the different polarised

channels. The displayed images are stretched by using a 4 sigma intensity interval (see section 2.3), so that the PWF images are less dominated by the speckle and more by the intrinsic contrast of the images. The PWF images therefore show more contrast between the fields. This is clearly an advantage for visual interpretation which is indicated by the better results of the *pwf* representation both in experiment A and B. In the single channel images urban areas show a relatively high scattering due to double bounce scattering from the buildings. Also forest shows a high scattering level due to multiple scattering, while water and some bare soil fields show a low scattering level due to single bounce flat surface scattering. Grass shows an intermediate scattering level due to a mixture of single bounce and multi-bounce scattering. The two-channel colour images show different colour tints for the bare soil fields and the urban areas or building complexes, compared to the other land use classes. This due to the fact that single and double bounce scattering do not give much scattering for the *hv* polarisation combination compared to the *hh* polarisation combination. The three channel colour images show in addition also different colour tints for the grassland. These additional colour tints probably depend on the grass height and the type of grass. Therefore they do not contribute to the discrimination between the land use classes used here and they are thus not of much help. This is confirmed by the results from experiment A and B, where the average score for the three colour channel representation is lower than for the 2 colour representation. This does not mean that a three-colour channel representation is not very useful. If one wants to discriminate for example between different types of low vegetation like crop types fully polarimetric data are indispensable.[3]

For experiment A the highest percentage of average correct classification is found for the *hhhv* representation (see Table 3) indicating that this representation is most effective for land use classification by visual interpretation. The *pol* representation has a lower average correct percentage, while the *hh* and the *pwf* representation show a significantly lower success rate. Inspection of the results presented in Table 3 shows that the *hhhv* representation gives significantly less confusion compared to the other representations.
Table 3 shows that most confusion is found for bare soil confused as grass, especially for the *hh* and *pwf* representation. Other important confusion is found for forest confused as grass, irrespective of the representation used. The confusion between bare soil and grass for the *hh* and *pwf* representations is due to the fact that the intensity levels for some fields are similar. For example bare soil fields with a rough surface and mowed grass can show the same backscatter in a single polarised channel. When however a colour representation (*hhhv* or *pol*) is used grass shows in general higher cross-polarised backscattering than bare soil fields and a better discrimination is obtained due to different colour tints, resulting in less confusion. The confusion between forest and grass is due to the fact that full-grown grass fields and young forest can show similar intensities and colours resulting in confusing. The confusion is more or less the same irrespective of the presentation used. Table 3 shows that grass itself does not show much confusion, irrespective of the representation used. This due to the fact the grass is used as background, covering 60% (see Table 2) of the scene.
On basis of intensity and colour it is surprising that there is not much confusion between urban and forest. The parts of urban areas, which are not dominated by strong double bounce scattering, often found for the smaller houses, show the same intensity and colours as forest. Next to intensity and colour, texture is important for visual interpretation of the images. In general texture is not very dominant in SAR imagery, since the speckle noise interferes with texture. However, when the resolution is high enough to see individual buildings and streets, texture is present in SAR imagery and allows discrimination between forest and these parts of urban areas.

For experiment B the low percentage of objects found in Table 4 shows that it is very difficult to detect objects in SAR imagery. The success rate is less than 11% except for the *hhhv* representation where a success rate of 27% is found. This relatively high score is due to the orange colour in combination with a high intensity. This appearance of the building complexes in the image is due to double bounce scattering. When building complexes do not give rise to such kind of scattering (e.g. not an appropriate aspect angle) it is very difficult to find buildings in the image. They are not or hardly present in the image. For the *pwf* representation the absence of colour is the main cause to have a low success rate, while for the *hh* representation the influence of speckle noise in the image makes it virtually impossible to discover the building complexes. The double bounce scattering shows a pink colour in the *pol* representation, which is apparently less obvious than the orange colour in the *hhhv* representation. The presence of more colour tints in the image for the *pol* representation produces more confusion and is a disadvantage for the task of finding buildings in the image. Therefore, the results are not better than for the grey tone *pwf* representation.

The polarimetric representation shows a lower success rate than the *hhhv* representation for both experiment B and A. The question arises whether the other polarimetric representations, the *physical* and *eigenwaarde* representation will show better results. Both the *physical* and *eigenwaarde* representations have a quite similar appearance when they are displayed. Main difference is the reduction in colour tints compared to the *sensor* representation used in the experiments, especially for the

land use class grass. Since these colours do not contribute to the discrimination between the land use classes they are not of much help. Therefore, use of these other representations might help to prevent confusion and for experiment A the absence of the confusing colour tints might enhance the results. However, there is no reason to expect a higher success rate for these representations than for the *hhhv* representation, because in combination with intensity and texture the number of colour tints in the *hhhv* representation is already sufficient to distinguish between the land use classes. Also for experiment B, the results for the other two polarimetric representations are not expected to be much better than the one obtained with the *sensor* representation. For all three coloured polarimetric representations the building complexes are coloured pink or purple, which is apparently a less effective trigger to find these objects, than the orange colour in the *hhhv* representation.

Apparently, for visual interpretation of SAR imagery, the use of only two uncorrelated coefficients σ_{hh} and σ_{hv} in two colour channels appears to be optimal. The extra information obtained by a fully polarimetric measurement is thus difficult to apply beneficially for human interpretation of SAR imagery. A fully polarimetric measurement gives a polarimetric covariance matrix with usually 5 parameters which all contain information. This is more information than is shown in the representations used in the experiments for visual inspection. To see whether this information can be applied to obtain better results we used an automatic classification procedure for fully polarimetric data. We applied this procedure to the same areas as used in the experiments A and B. We used a supervised procedure by determining average covariance matrices from the data by selecting training areas, which are typical for the land use classes and the building complexes. In case of experiment B we used the covariance matrix which is typical for grass as background. For the classification the following discriminant function was used: [4]

$$D_k = trace(C_k^{-1}C) + \ln |C_k| \tag{10}$$

where C_k is the covariance matrix typical for class k and C is the covariance matrix of the pixel to be classified. A land use class k is assigned to that pixel when the discriminant D_k is a minimum. For obtaining C we used the averaged covariance matrix of 3x3 pixels to reduce the influence of speckle.

In this way, for the area in experiment A, a classification result is obtained with much confusion between urban areas and forest, since for parts of urban areas without double bounce scattering, the polarimetric covariance matrices resemble those of forest. The only way to distinguish between these urban areas and forest is the use of texture since urban areas show much texture due to streets and buildings, while forest does not. Therefore, as a last step in the classification procedure we reclassified forest to urban when the local texture was above a certain threshold. To obtain texture information we calculated a texture image using the PWF image averaged over 3x3 pixels. Next we obtained the texture measure by calculating the ratio of the standard deviation over the mean in a window consisting of 5x5 averaged pixels group. A texture cell therefore has the dimensions of 15 x 15 original pixels, i.e. 45 meters. The result is shown in Figure 4, where also the final classification result is shown.

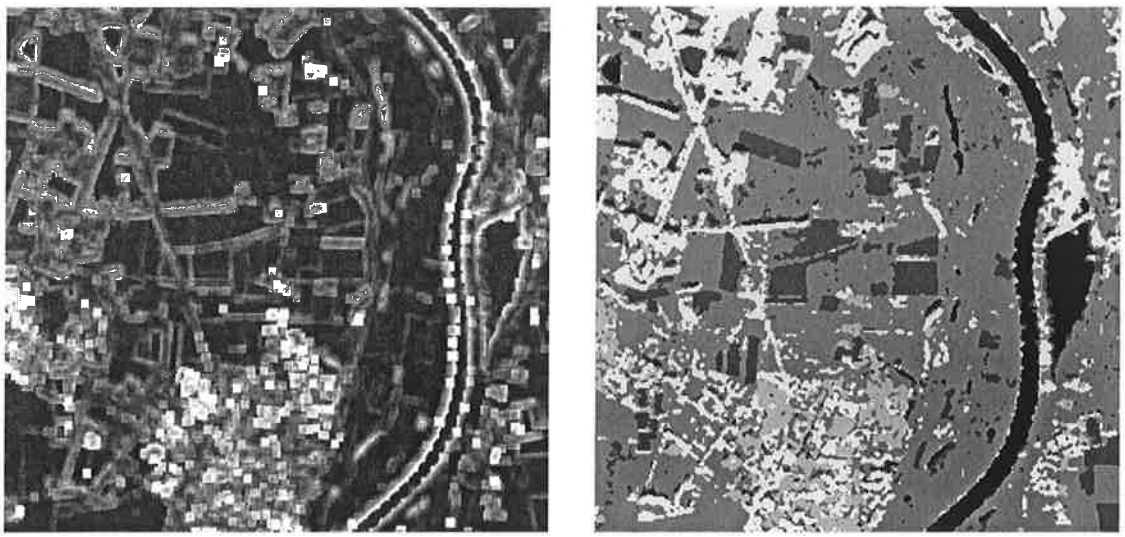

Figure 4. Left the texture image is shown and right the classification results from the automatic procedure. Land use classes as in Fig. 2.

To be able to compare this result with the results from the visual inspection we calculated the confusion matrix from the automatically classified image and the reference template of experiment A. The confusion matrix shown in Table 5.

Table 5. Confusion matrixes for the automatic classification procedure in experiment A

Automatic classification	Bare soil	Water	urban	Grass	Forest
Bare soil	66	1	0	30	2
Water	9	65	2	18	6
Urban	4	1	29	37	30
Grass	8	2	2	78	11
Forest	4	1	2	28	64
Average correct 60%					

Inspection of Table 5 and Figure 4 shows that still much urban areas are classified as forest and grass. Other significant confusion is found for bare soil classified as grass and forest as grass. The confusion makes that the average percentage of correct classification is lower for the automatic procedure that for the visual interpretation of the *pol* representation. Apparently people are better able to distinguish between land use classes than an automatic procedure is able to do.

For the area of experiment B only two classes were applicable: building complexes and background. Analogously to experiment A we obtained a classification result, which has been compared with the reference template of experiment B. We found that about 90% of the objects were detected by the automatic procedure, but also many objects were detected falsely, mostly forest edges. Therefore, an automatic procedure is more effective for the detection of objects in polarimetric SAR imagery than visual inspection, although 'false' detection is a problem.

To enhance the results for finding objects in a polarimetric SAR images we can make use of the fact that objects usually show high backscattering due to single or double bounce scattering. The logarithmic scaling in dB and the four sigma stretching (see equation 8 and 9) make that in the displayed image the general background is more prominent at the expense of the visibility of objects. This obviously hinders the discovery of objects in case of visual inspection. Therefore, for the purpose of finding objects in SAR imagery it would be advantageous not to stretch the image in dB and use a manually adjustable intensity stretching to display the image. Polarimetric data allow calculating which polarisation combinations give maximum contrast between an object and its background.[5] This technique, called contrast optimisation, can also be used for more effectively detecting objects in polarimetric SAR imagery.

5. CONCLUSIONS

People are reasonably successful in performing land use classification using SAR data. Multi-polarised data are therefore required, but these data need not to be fully polarimetric. Good results were obtained with *hh*- and *hv*-polarisation combinations, displayed in the red and green colour channel, respectively. Finding objects in SAR imagery by visual inspection is very difficult. Most representations gave minimal results. Only when the *hh*- and *hv*-polarisation combinations were displayed in the red and green channels, somewhat better results were obtained. We therefore conclude that the *hh* and *hv* polarisation combinations displayed in the red and green channels, is the most effective one of the representations studied for visual interpretation of SAR imagery. An important property of the *hh* and *hv* polarisation combinations is that they are not correlated for most objects and land use classes, so that colour tints are optimally obtained. For an operational context this combination is important since the measurements can be done with a simpler SAR sensor than a fully polarimetric SAR sensor. Next to the dual polarised receiving antenna only a single polarised transmitting antenna is needed. There are no reasons to believe that other representations of fully polarimetric data (*physical* representation or *eigenwaarde* representation) than the one (*sensor* representation) used in the experiments will give significantly better results for visual interpretation of SAR imagery. Compared to an automatic classification procedure, land use classification by visual inspection appears to be the most effective. Automatic detection of objects gave better results than detection by visual inspection, but many false objects were also detected. In order to improve the success rate for detecting objects in SAR images by visual inspection other techniques like contrast optimisation or dynamically adjusting intensity levels for displaying polarimetric SAR data might be helpful.

ACKNOWLEDGEMENTS

The Dutch Ministry of Defence has partly sponsored the work presented in this paper.

REFERENCES

1. S.V. Nghiem, S.H. Yueh, R. Kwok, and F.K. Li, "Symmetry properties in polarimetric remote sensing", *Radio Science,* **27**, *No. 5*, pp. 693-711, 1992

2. L.M. Novak, and M.C.Burl, "Optimal speckle reduction in polarimetric SAR imagery", *IEEE transactions on Aerospace and Electronic Systems,* **26(2)**, pp. 293-305, 1990

3. A.C. van den Broek, J.S. Groot, "Classification and soil moisture determination of agricultural Fields", *Summaries of the Fourth Annual JPL Airborne Geoscience Workshop October 25-29, Washington, JPL publication,* **93-26**, pp.77-80, 1993

4. J.S. Lee, M.R. Grunes, and R. Kwok, "Classification of multi-look polarimetric SAR imagery based on complex Wishart Distribution" , *Int. J. RS.,* **15**, *no. 11*, pp. 2299-2311, 1994

5. A.A. Swartz, H.A. Yeuh, J.A, Kong, L.M. Novak, and R.T. Shin, "Optimal polarisations for achieving maximum contrast in radar images", *Journal of geophysical research,* **93**, *no. B12*, pp. 15,252-15,260, 1988